

WASTE HEAT RECOVERY ON TRACTOR ENGINE: EXERGY ANALYSIS OF EXHAUST IN TRANSIENT CONDITIONS

Stephanie LACOUR^{1*}; Sylvain DESCLOUX¹; Franscesco BALDI¹; Pierre PODEVIN²

1 Laboratoire de génie des procédés pour l'environnement, l'énergie et la santé (LGP2ES-EA21), Irstea, 1 Rue Pierre-Gilles de Genne, CS 10030, F-92761 Antony cedex

2 Laboratoire de génie des procédés pour l'environnement, l'énergie et la santé (LGP2ES-EA21), Cnam, case 2D3R20, 292 rue saint Martin 75003 Paris – France

Abstract: Waste heat recovery (WHR) systems are an interesting way to improve the efficiency of internal combustion engines and reduce their fuel consumption for a given mechanical output. Exergy analysis is used to quantify the maximum amount of mechanical energy that could be recovered in the exhaust gases, i.e. the potential for recovery. In this paper, measurements are carried on a diesel tractor engine in order to assess this potential. We also measured the energy transferred in a secondary fluid through a heat exchanger placed in the tailpipe. First, a "steady state" map of exhaust gas exergy is computed for various operating conditions. It shows the great interest of waste heat recovery systems for tractor engine, because the highest potentials are observed for high load factors, the most frequent operating conditions. Then, we developed driving cycles in order to simulate an intermittent power demand similar to real use. The instantaneous exhaust exergy is always related to the instantaneous fuel exergy with a small delay. For cycles with constant engine speed, the exhaust gas exergy is, in average, proportional to the mechanical output work and to fuel exergy. But the thermal inertia influences the exhaust exergy, leading to a better recovering ratio when the power demand decreases and heat is desorbed. Moreover, measurements point out that the WHR potential is reduced during acceleration phases. Exhaust gas exergy grows slowly during acceleration because of the combined effects of lower temperature and air flow growths in this step. During deceleration, the recovery potential is therefore higher than in acceleration. The average potential in time is not sensitive to signal period and power range, but it is reduced of 20-30% when compared to a steady state assessment. In the secondary fluid circuit, a linear relation is observed between the exhaust gases exergy and the heat transferred to the cold fluid. Differences between acceleration and deceleration also appears leading to 10% more in the heat transfer during deceleration step.

Keywords: exergy, exhaust gas, transient driving cycle, inertial effect, recovery potential

INTRODUCTION

Fuel oil resources are vanishing and efforts are made both to look for alternative fuels as well as to increase energy efficiency of mobile applications. In parallel, the energy efficiency concept evolves to handle more accurately with the second law analysis through exergy approaches.

The exergy of a fluid, also called availability, is the maximum useful work produced if the system reaches its chemical, thermal and mechanical equilibrium with the surrounding(1). Rakopoulos and Giacoumis have reported in (2) findings on exergy or availability analysis on internal combustion engine (ICE). The majority of works have focussed on the dominant combustion irreversibilities: benefits of high combustion temperature or reducing excess air are discussed for in-cylinder operations from the first and second law efficiency. It is shown how all the parameters which increase the level of pressure and temperature lead to a reduction of combustion irreversibilities. Few studies are related to the engine subsystem irreversibilities. If the exergy concept has given some interesting guidelines about fuel choice and engine design, it is also very meaningful to apply it on waste heat recovery topics (WHR) (3).

* Corresponding author. Email: stephanie.lacour@irstea.fr

Using both energy and exergy analysis, Bourhis (4) examined the exergy distribution in diesel and gasoline engines. He showed that between 4 and 9% of the fuel exergy could be recovered in exhaust gases and transform into mechanical work through a secondary engine. Many techniques are proposed as secondary engine, like turbocompounds, rankine engines or thermoelectric generators. Armstead and Miers examine in (5) these methods for converting waste heat recovery into work. They notably stressed that thermal power sources in automotive applications are highly dynamic, what could affect the performance of a real WHR system. Models are often used to assess the potential of waste heat recovery ((6) (7), (8)). Rankine organic cycle, one of the most popular techniques in WHR, is expected to improve engine efficiency of 3-5%. But all these authors stressed the uncertainties of the improvement in transient conditions and so are the real driving conditions.

In this paper, we aim to present some contribution in exergy approach applied to transient driving of an ICE. As we are interested in tractor engine, specific driving cycles were developed in order to deal with the specific use of these engines. These cycles enable us to understand better the WHR in the exhaust gas of a diesel engine submitted to transient power demand. Using steady state and transient driving cycle, we made measurements with an experimental set up that is presented in the second section. The exergy of exhaust gases is then assessed from bench tests measures and results are discussed in the following section. Steady state results are first examined. Then, the transient exergy is assessed and we looked for the relation between the instantaneous mechanical power, fuel and exhaust exergies. The average values of these variables are also presented and compared to the steady state values. At the end, the instantaneous heat transfer is observed for growing and decreasing power demand.

TESTING METHODS

Diesel engines for agricultural machinery have their own typical features during use and this latest differs a lot from other vehicles. Tractors engine are generally used with load coefficient around 60%, what is much higher than the typical load of passenger car engines (17%). For both applications, the power demand also fluctuates along the use. The most typical feature of a tractor engine is the fact that engine power is not strictly related to tractor displacement: the engine crankshaft is connected to gearbox, but also to a second shaft named power-take-off allowing moving agricultural implements. For in-field operations, the engine power is used both for displacement and implement work. Furthermore, the engine speed sometimes needs to be constant, in order to ensure optimal implement work. Then, the power demand is relatively constant and high during displacement along the furrow and is interrupted at the end to make the about turn. This appears clearly on the engine parameters we have recorded along a day dedicated to sugar beet harvesting (Figure 1). During road driving, at the end of the day, the mechanical power delivered by the engine is much more transient: if the average of the power demand is lower than for in-field, the instantaneous values exhibit an important scattering, even if tractor velocity is low compared to other road-vehicles.

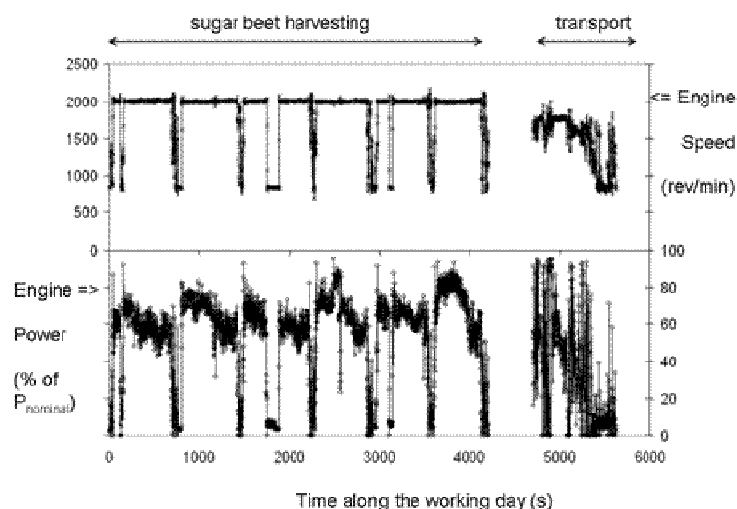


Figure 1. Engine speed and power recorded on field during tractor operation along a day

Although the shape of power demand is near a Heaviside function, we preferred, for practical reasons, to use a sinusoidal function to represent the alternation of low and high demand during tractor use. In some case, engine speed was kept constant and the torque follows the sinus law. In the cycle 5, both torque and engine are controlled with the following expression:

$$G(t) = \bar{G} \sin(\omega t)$$

Table 1 . Parameters of driving cycles used for testing engine

Cycle	Period ω	Average Power	Power range	Average Engine Speed	Engine speed range
	(s)	(kW)	(kW)	(rev/min)	(rev/min)
1	300	29	0-58	2350	-
2	300	29	6-52	2100	-
3	300	29	14-43	2100	-
4	300	29	-	2050	2000-2100
5	300	26	0-58	1400	800-2100
6	70	29	0-58	2350	-

6 driving cycles were tested in this work and their characteristics are detailed in Table 1 . These cycles were used for bench tests of a tractor.

MATERIAL

Tractor tests are conducted at the Cemagref bench test facilities. The experimental set-up is described in the Figure 2. The vehicle used in this experiment is a tractor Renault 851-4R equipped with a diesel engine, direct injection. This tractor is coupled through the power-take-off (PTO) at a dynamometer Schenck W400. The engine has four cylinders, whose capacity is of 4.165 l and is equipped with a turbo compressor: it develops a PTO power of 60 KW at 2350 rev/min. The PTO power is measured and considered here as the mechanical output work of the engine

The tractor is fuelled with domestic fuel oil: temperature and flow are monitored. An additional heat exchanger is located in the exhaust pipe: this is the secondary fluid circuit. It consists in a simple duct made of copper of 37.5 cm length and 0.8 cm of internal diameter. The secondary fluid is the water distributed by the local water network. A flow analyser, HORIBA OBS2200, is positioned after the heat exchanger: it measures airflow, temperature and gas composition (NOx, CO, CO2, THC).

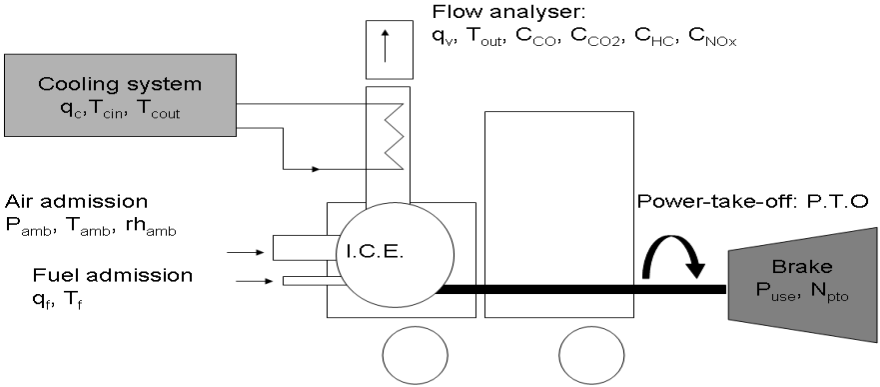


Figure 2. Experimental set-up for testing tractor engine

Driving cycles were used to assess the brake effort and acceleration amount during the tests. The whole set of variables described in Figure 2 is recorded and used to assess the exergy balance of the engine.

The exergy input in the system is assessed using the following relation:

$$Ex_{fueli} = \rho(T_f) \cdot q_{vf} ex_f + \rho(T_{amb}, rh_{amb}) \cdot q_{v,air} ex_{air}(T_{amb}, rh_{amb})$$

Assuming 42.24 MJ/kg as low heating value and β values of 1.1 ((9), (10)), the specific exergy of fuel was set to 46.93 MJ/kg. The ambient air exergy was taken into account but it represents less than 0.1% of the exergy input. The air exergy was computed from the intake air flow, neglecting air pressure and taking account of the air humidity (rh) by the Rankine formula.

In the exhaust, the gas composition (CO₂, N₂, O₂, H₂O) was used to compute the mass fraction of each components, as well as the specific heat capacity and then, entropy of the mixture. Other pollutants were neglected in the exergy and heat exchange in the tailpipe was supposed to be at constant pressure.

$$Ex_{ex} = \int_{T_0}^{T_{ex}} \rho(T_f) \cdot q_{vf} C_p(Y_i, T) \left(1 - \frac{T_0}{T}\right) dT$$

Table 2. Polynomial coefficients used for heat capacity assessment of exhaust gases mixture

$C_p = a_0 + a_1 T + a_2 T^2 + a_3 T^3$				
(J/kgK)	a_0	a_1	a_2	a_3
CO2	0.451	1.91e-3	-1.79e-6	7.39e-10
H2O	2.94	-6.81e-3	1.42e-5	-9.09e-9
O2	0.973	-6.35e-4	1.89e-6	1.24e-9
N2	1.09	-3.11e-4	5.71e-7	1.43e-10

The reference or dead state is dry air at 1 bar and 273 K for the exergy input and output. Hence, the chemical exergy of the exhaust gases is neglected. The reference temperature is not the usual one (in general, 298K) but it is used here because of the cold fluid (water at the exchanger entry) is above 298 K: it was easier in our calculations to deal with positive exergies by decreasing the reference temperature below 9°C. By this way, we had only positive exergies and we assumed to produce exergy values slightly higher than in the literature.

RESULTS

Steady state exergy

A preliminary test was made according to the OECD code for agricultural machine: this code is a normalized test procedure use to produce the power assessment of tractors. This test is somewhat equivalent to regulation tests (FTP or 13-modes) used for pollution assessment, excepted that it is realized on the complete vehicle and not only on the engine. The operating points are also different and are more in relation with agricultural operation in the OECD code. In this procedure, the P.T.O power and fuel consumption are measured after 3 min of stabilization phase. It is considered here as the stationary case.

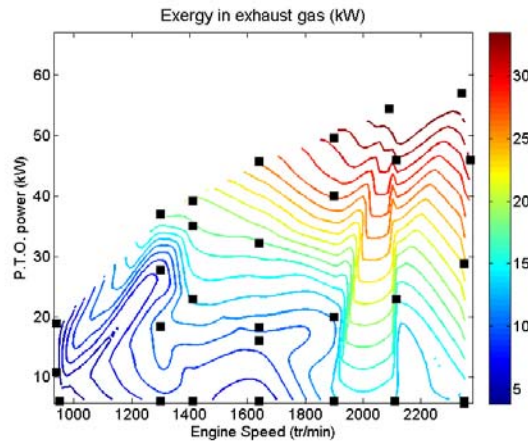


Figure 3. Exergy content of exhaust gases in the tail pipe of a tractor in steady state conditions

The recoverable energy potential is assessed by the exergy content of flows, depending on operating conditions, as shown on Figure 3. The exergy behavior shows the same shape than those presented in (11) for light-duty vehicles. The potential for recovery is high, about 35 kW for the maximal value: this represents about 15% of the fuel exergy and 60% of the mechanical energy delivered by the engine. The potential slightly increase with engine speed, but exhibits a large increase with the P.T.O. power. The maximum potential is reached near nominal conditions (2350 rpm, 57.6 kW). As the waste heat recovery potential is growing with the load factor, a recovery subsystem is obviously very interesting for this kind of applications, where both engine powers and load factors are generally high.

Transient exergy of exhaust gases

Then, the driving cycles described earlier are tested and results are presented in the Figure 4. In the left top picture, the power dissipated in the brake exhibits the trigonometric behavior. In the left bottom and right pictures, the exhaust exergy varies in relation with the P.T.O. power as well as with the fuel consumption (not shown in this paper). The behavior is quite similar for all of the cycle represented in the right figure. Only the cycle 4 differs because it is based on constant P.T.O. power. For other cycles, the exergy of exhaust gases increases more slowly than the mechanical energy when the power increases. It also decreases more slowly than the mechanical output in power descending phase. This is why we observed such an ellipse on the graph. For the cycle 1, 2, 3, the ellipse is quite symmetrical: these are constant engine speed cycles where the air flow rate stays roughly constant. Therefore, the delay between the mechanical power and the exhaust exergy should be attributed to the temperature effects. This is why the width of the ellipse is related to heat adsorption and desorption to the air flow along the pipe: it marks the difference between power increase and power decrease and it is therefore the shape of transient effects. The larger range has the input signal, the more width the ellipse is. For cycle 6 (in red), the ellipse presents larger differences between the acceleration and deceleration step. This is mainly due to difficulties in controlling the brake parameters in the fast cycle. The biggest difference of exergy between acceleration and deceleration step is observed on cycle 5, where both torque and engine speed varies along the time. This appears more clearly on the bottom left graph. The link between exhaust exergy and mechanical power is nearly linear during the deceleration step (above the ellipse). This linearity disappears in the acceleration step (below the ellipse). The non linear relation is the outcome of both fuel exergy variations and air flow rate variation: the air flow increases with a lower rate during the acceleration phases than in deceleration phases. This might be related either to the strong mechanical inertia of the engine or turbo charger effect.

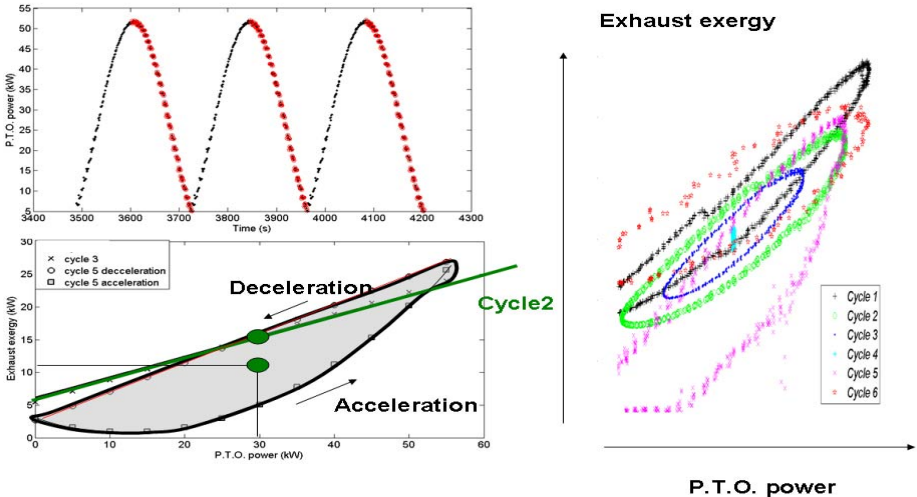


Figure 4. P.T.O. power along the time and associated exhaust gases exergy on driving cycle 5 (left) and for the whole set of driving cycles (right)

The mechanical power and the exergies of exhaust and fuel were integrated over each period of the cycles and results are given in Table 3 and presented on the Figure 5. The average exergy (respectively

power) is the representation of exergy on the whole cycle. The exhaust exergy is compared to steady state values (number in parenthesis). This latest is deduced by the interpolation of the exergy measured for $(\bar{N}_{cycle}, \bar{P}_{cycle})$ in the steady case. The gap between the steady state and transient exergy fluctuates between 23 to 30%. The average value for transient cycle is always below what we defined as the "steady state exergy", indicating that's the transient availability is lower than the steady one. From the figure, we notice that the averages remain constant: only small variations, generally related the room temperature changes, affects our values. Measurements are very reproducible, excepted for cycle 6.

Table 3. Average exergies over the cycle (6 periods)

Cycle	Fuel Exergy (kW)	Mechanical Power (kW)	Mechanical Efficiency (%)	Exhaust exergy (kW)	Exergy ratio (% of fuel)	Exergy ratio (% of PTO)
1	133.7	28.6	0.21	18.0 (23.3)	0.13	0.63
2	96.0	28.8	0.30	15.1 (19.6)	0.16	0.53
3	100.9	28.7	0.28	15.0 (19.6)	0.15	0.52
5	68.7	25.8	0.38	10.7 (15.4)	0.16	0.42
6	106.2	28.5	0.27	18.0 (23.3)	0.17	0.63

Looking first at fuel exergy, the average value is very high for the cycle 1, although the mechanical output is near those of cycles 2 and 3. This is because we used a very high engine speed for this cycle. In this case, the diesel engine efficiency is lower than in other cases. Therefore, the fuel exergy needed for the same power output is higher. But the availability in the exhaust is also lower in this case, what is not explained.

The cycle 6 is very similar to cycle 1, excepted the shorter period of the signal. Comparing cycle 1 and 6 shows that the period of the signal affects very slightly output exergies on average.

Then, comparing cycles 2 and 3, results appears very similar: this indicates that the range of the transient torque has only a little influence on the averaged values.

For cycle 5, the exhaust exergy, fuel exergy and mechanical power are the lowest. However, the exergy ratio, related to fuel, is in the same order of magnitude than for the cycles 2 and 3. It suggests that the average recovery potential doesn't decrease a lot for this cycle with transient torque and speed, compared to the other cycles with transient speed only. The power efficiency of the diesel was found very high for this cycle and it explain the poor exergy to work ratio.

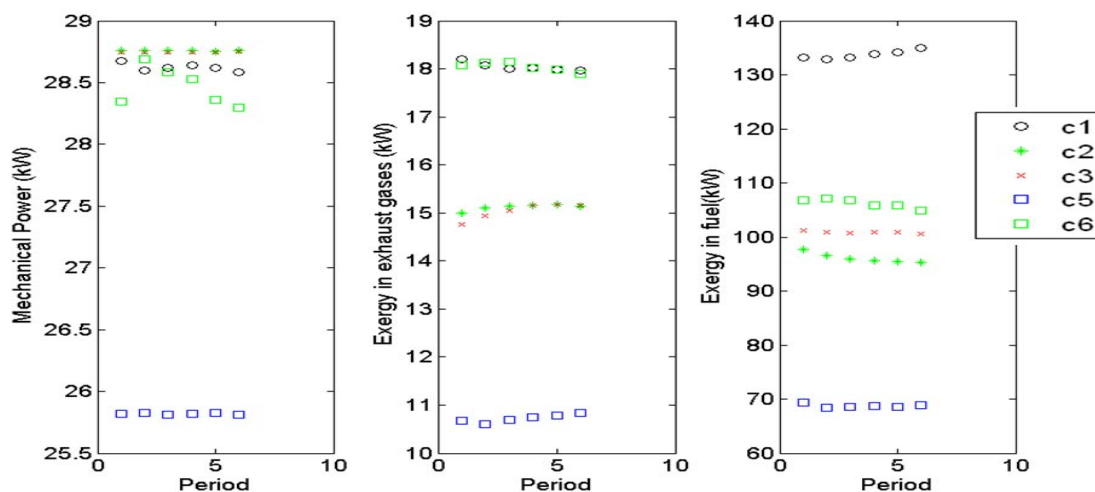


Figure 5. Mechanical power, exergy of exhaust and fuel over periods for different driving cycles (kW)

From a cycle to another, the ratio of exergy to power was found to be more sensitive on cycle than the ratio exhaust exergy to fuel exergy. It is therefore a poorer indicator of the WHR potential.

Losses within the heat exchanger

A heat exchanger is located within the tailpipe. Some water comes in the exchanger with a very low and constant temperature and is heated by exhaust gases. The water flows is nearly constant. Results of the heat transferred from the exhaust gases to water are presented in Figure 6. The average energy transferred to water is around 560 W for cycle 1, what is about 60% of the gas energy losses across the exchanger. Other losses occur through the tailpipe because of the lack of thermal insulation in our experimental set up. We assumed in the analysis that the water energy is the effective heat recovery and it should be compared to the exhaust exergy, theoretical maximum of potential. The heat received by water is in relation with both fuel exergy and exhaust availability. For a given fuel availability, the amount received by water is smaller if the power demand is increasing. This is because the growth of the fuel consumption is dedicated the increase of both mechanical and thermal energy, fighting about the inertia. In the decreasing step, both thermal and mechanical inertia allows a higher P.T.O. power for a given fuel consumption. In the same way, the recovered heat is also higher during this step.

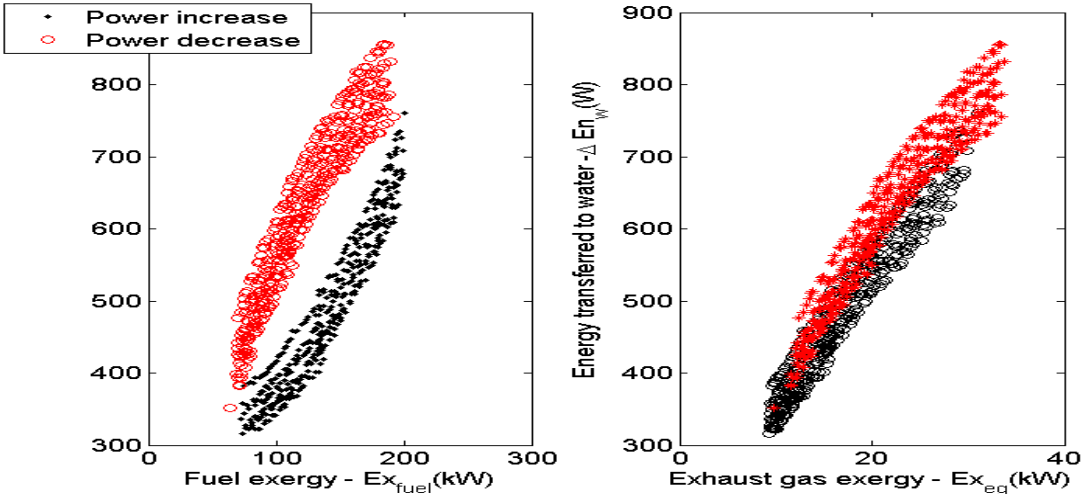


Figure 6. Net energy received by water through the exchanger according to fuel exergy (left) and exhaust gas exergy (right) on cycle 1

The gap between the "power increase" and "decrease step" is less sensitive on the right figure. Here, the link between the exhaust exergy and the water energy is quite linear. Exhaust exergy is therefore a better indicator of the recovery potential than the fuel exergy, because it is not sensitive to some non linear effect of the first and main engine. But even in that case, it is shown that thermal absorption and desorption has an effect on the real recovery. For a given exhaust potential, the heat transfer is increased of roughly 10 % in the decreasing power step.

CONCLUSION

In this paper, the transient driving effect on the heat recovery potential is assessed on a diesel engine. Some specific driving cycles were developed in order to simulate operating intermittencies related to tractor use. The experiments were carried on the tractor test bench facilities of Cemagref. A steady state map of exhaust exergy was built up for steady state measurements. It shows that exhaust potential for a secondary engine is very high, especially when expressed in relation to the mechanical power, i.e. the main parameter for this kind of applications. Then, transient cycles were studied and the gap between instantaneous exergies during decreasing or increasing power demand appears clearly in our results. For cycles with regulated engine speed, the recovery potential was always interesting because exhaust flow rate remains high, whatever the power demand. When both engine speed and torque vary, the gap between exergies in acceleration and deceleration steps is amplified. That is coming from both gas temperature and flow rate variation. By integrating the values, it is found that the transient potential is 23 to 30% less than the steady potential. Finally, the real energy recovery through a heat exchanger is compared to fuel and exhaust exergies. It is shown that transient effects

were also observed on the heat transfer, leading to a higher energy recovery in deceleration, compared to the one during acceleration. The increases for deceleration are supposed to be related to heat desorption in the engine. But the transient effects are less sensitive on the exchanger, because the recovered energy differs of around 10% between acceleration and deceleration phases. On contrary to fuel exergy, exergy in the exhaust gases was found to be a linearly related to heat transfer in the secondary fluid. Further work is needed on to better understand the effect of accumulated heat on the recovery potential for the highly intermittent engines.

REFERENCES

1. L. Borel, D. Favrat, *Thermodynamique et énergétique: de l'énergie à l'exergie*. EPFL, Ed. (PPUR, Lausanne, 2005), pp. 805.
2. C. D. Rakopoulos, E. G. Giakoumis, *Progress in Energy and Combustion Science* **32**, 2 (2006).
3. K. K. Srinivasan, P. J. Mago, S. R. Krishnan, *Energy* **35**, 2387 (2010).
4. G. Bourhis, P. Leduc, *Oil Gas Sci. Technol - Rev. IFP* **65** (Janvier-Février 2010, 2010).
5. J. Armstead, S. Miers, paper presented at the Internal Combustion Engine Division Fall Technical Conference (ICEF2010), San Antonio, Texas 2010.
6. P. J. Mago, K. K. Srinivasan, L. M. Chamra, C. Somayaji, *International Journal of Energy Research* **32**, 926 (2008).
7. Y. Dai, J. Wang, L. Gao, *Energy Conversion and Management* **50**, 576 (2009).
8. A. Abusoglu, M. Kanoglu, *Applied Thermal Engineering* **29**, 242 (2009).
9. Y. Kalinci, Hepbasli A., Dincer, I., *Int. J. of hydrogen energy* **34**, 8799 (2009).
10. L. Talens Peiro, G. Villalba Mendez, X. Gabarrell i Durany, *Environ Sci Technol* **42**, 4977 (2008).
11. K. D. Edwards, R. M. Wagner, paper presented at the Internal Combustion Engine division Fall - ICEF2010, San Antonio, Texas, USA 2010.